DOI: 10.1002/adsc.201201047

Palladium N-Heterocyclic Carbene Catalysts for the Ultrasound-Promoted Suzuki–Miyaura Reaction in Glycerol

Arturo Azua,[a] Jose A. Mata,[a,*] Pauline Heymes,[b] Eduardo Peris,[a] Frederic Lamaty,[b] Jean Martinez,[b] and Evelina Colacino[b,*]

[a] Departamento de Química Inorgánica y Orgánica Universitat Jaume I, Avda. Sos Baynat s/n, 12071 Castellón, Spain
Fax: (+34)-96-438-7522; phone: (+34)-96-438-7516; e-mail: jmata@uji.es
[b] Institut des Biomolécules Max Mousseron (IBMM), UMR 5247 CNRS – UM I-UM II, Université Montpellier II, Place E. Bataillon, 34095 Montpellier Cedex 5, France
Fax: (+33)-(0)4-6714-4866; phone: (+33)-(0)4-6714-4285; e-mail: evelina.colacino@univ-montp2.fr

Received: December 18, 2012; Revised: February 21, 2013; Published online: April 8, 2013

Supporting information for this article is available on the WWW under http://dx.doi.org/10.1002/adsc.201201022.

Abstract: Novel palladium N-heterocyclic-carbene (NHC)-based complexes with 3,4,5-trimethoxybenzyl, alkyl and sulfonate N-substituents were obtained and fully characterized. The new complexes were used as pre-catalysts in the Suzuki–Miyaura coupling of various aryl halides/boron sources in glycerol under pulsed-ultrasound (P-US) activation. High yields were obtained under mild reaction conditions, without formation of undesired by-products. The pure final cross-coupling products were easily recovered without column chromatography and the catalytic/solvent system could be recycled. TEM (transmission electron microscopy) and XPS (X-ray photoelectron spectroscopy) were used to characterize the nanoparticles and to investigate the fate of the catalysts.

Keywords: green chemistry; glycerol; N-heterocyclic carbenes; sonication; Suzuki–Miyaura reaction; XPS; X-ray photoelectron spectroscopy

Introduction

One of the major challenges in academia and industry point in the direction of reducing environmental impact of chemical processes, through a chemistry '*benign by design*'.[1,2] In this context, substitution of volatile organic solvents with new sustainable media,[3] energy saving[4–6] and selective protocols for catalytic and organic processes is nowadays an active research area. The replacement of solvent derived from fossil oil reserves or from bio-mass is a matter of great economic concerns. This context is boosting the renaissance of glycerol, with the conversion of natural lipids into biodiesel switching its role from waste to an economically, viable and eco-friendly solvent,[7–9] or even as a substrate for the production of higher value-added chemicals.[10–12] In the field of palladium-catalyzed processes, two seminal papers have recently described the Suzuki–Miyaura cross-coupling reaction in glycerol at 80 °C under microwave[13] or continuous ultrasound[14] activation. These two studies demonstrate the superiority of these alternative energy inputs with respect to oil-bath heating for one model reaction, which was catalyzed by a phosphine-based palladium species. Efficient heating of the reaction medium is achieved under microwave activation because of the high dielectric constant of glycerol. However, the process suffers from catalyst deactivation due to the formation of palladium black. Ultrasound activation allows the overcoming of one of the main drawbacks in the use of glycerol due to its high viscosity, limiting mass transport and efficient mixing of the reaction mixtures. Unfortunately, an investigation of the homocoupling or dehalogenation by-products is not mentioned, while substrate scope and recycling of catalyst-solvent system also remain unexplored. We report herein the use of glycerol, as the reaction solvent for the Suzuki–Miyaura cross-coupling reaction catalyzed by four newly prepared N-heterocyclic carbene (NHC) palladium complexes under pulsed ultrasound activation (P-US). Results were compared to those obtained with PEPPSI (pyridine enhanced precatalyst preparation stabilization and initiation)-IPr pre-catalyst[15–17] (Figure 1). The fate of the catalyst at the end of the process was also investigated through transmission electronic microscopy (TEM) and X-ray photoelectronic spectroscopy (XPS). In order to provide more useful information

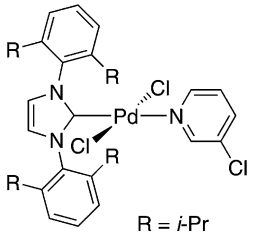

Figure 1. PEPPSI (pyridine enhanced precatalyst preparation stabilization and initiation) type catalyst.

about the potential use of this alternative energy input over palladium-catalyzed chemistry, we studied the substrate scope of the process, we investigated whether any undesired by-product was formed in the reaction course, and we also explored the possibility to recycle the solvent/catalyst system.

Results and Discussion

Palladium(II) complexes of the general formula $[PdCl_2(NHC)Py]$ **1–4** (Scheme 1) were prepared in good yields starting from $PdCl_2$ and the imidazolium salts **A–D**, using potassium carbonate in pyridine at 60 °C, following a similar synthetic protocol as previously described for the preparation of other related Pd(NHC)Py complexes.[18–20] The imidazolium salts **A–D** were readily accessible by alkylation of commercial available *N*-alkylimidazoles following already described procedures.[9,21–23]

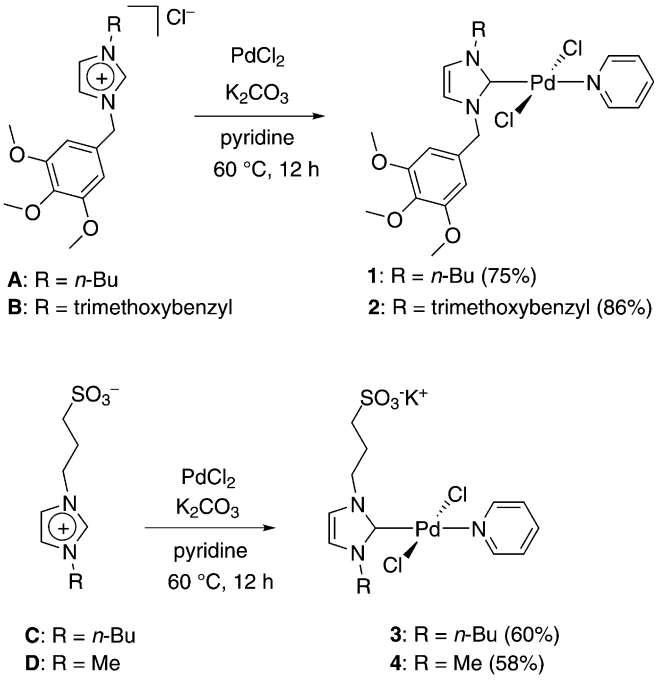

Scheme 1. Palladium(II)-NHC based complexes.

The palladium(II)-based complexes are pale yellow solids stable both in the solid state and in solution. Complexes **1** and **2** were soluble in solvents such as dichloromethane and chloroform, and partially soluble in glycerol,[24] while complexes **3** and **4** were only soluble in polar solvents such as methanol, water and glycerol. Complexes **1–4** were characterized by NMR, mass spectroscopy and elemental analysis. The most relevant feature of the ^{13}C NMR spectrum of **1** and **2** were the signals due to the metallated $M-C_{carbene}$ carbons at 153.5 (for **1**) and 153.6 (for **2**) ppm. ^{13}C NMR signals assigned to the metallated carbons of **3** and **4** appeared at 152.8 and 152.1 ppm, respectively. High-resolution mass spectroscopy (HR-MS) analysis of complexes **1–4** showed a good agreement between the simulated and theoretical spectra with relative errors inferior to 1 ppm, confirming the proposed nature of these complexes (see the Supporting Information for details).

X-Ray Diffraction Studies

Crystals of complex **1** suitable for X-ray diffraction were obtained by slow evaporation from concentrated dichloromethane-hexane solutions. Figure 2 shows the molecular diagram of the palladium complex with the atom numbering and the selected bond lengths [Å] and angles [°]. Crystal data and structure refinement are described in the Experimental Section and the

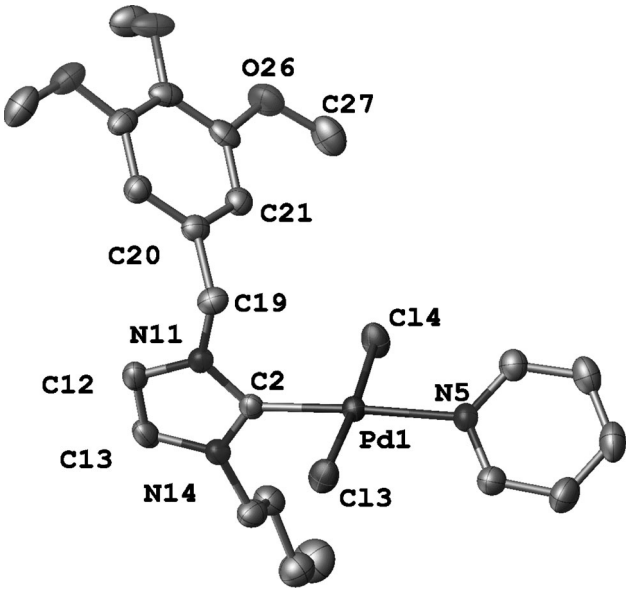

Figure 2. X-ray structure of complex **1**. Ellipsoids at 50% probability level. Selected bond lengths [Å] and angles [°]: Pd(1)–C(2) 1.958(3), Pd(1)–Cl(3) 2.3021(8), Pd(1)–Cl(5) 2.3018(8), Pd(1)–N(5) 2.199(2), C(2)–Pd(1)–Cl(3) 88.13(8), C(2)–Pd(1)–Cl(4) 87.96(8), Cl(3)–Pd(1)–Cl(4) 176.05(3), C(2)–Pd(1)–N(5) 175.87(10), N(11)–C(2)–N(14) 105.7(2).

Supporting Information. The geometry at palladium of **1** was square planar with two chlorides in a *trans* disposition, one NHC and a pyridine. The palladium coordination plane was almost perpendicular to the plane angle defined by the azole ring ($\alpha = 81.1°$). The Pd–$C_{carbene}$ bond length was 1.958(3) Å. The (trimethoxy)benzyl group was pointing away from the palladium just avoiding steric repulsion.

Catalytic Studies

Palladium complexes bearing N-heterocyclic carbene ligands are excellent catalysts, especially in carbon-carbon bond formation reactions with the PEPPSI-type palladium complexes being particularly active in the Suzuki–Miyaura reaction.[17,25–28] In this perspective, complexes **1**–**4** were evaluated for their activity in an unusual solvent such as glycerol under unexplored pulsed ultrasound activation. Catalyst **1** was used for a preliminary screening of the reaction conditions (Table 1). Reactions were carried out with a 1 mol% of catalyst loading at 40 °C. *p*-Iodo- and *p*-bromoanisole were used as benchmark substrates to screen the suitable reaction conditions. Two different ultrasound irradiation modes were tested: continuous (referred to as C-US) or pulsed (referred to as P-US). During a continuous irradiation mode, constant cavitation phenomena occurred during a period of 10 min. With pulsed ultrasound mode, cavitation is promoted every ten seconds (followed by 10 seconds in which the probe is swiched off), during 30 min. In this way, the effective time during which the sample is irradiated corresponds to 15 min, which remains comparable in terms of time to the conditions used under the continuous mode (10 min). With the *p*-iodoanisole/$PhBF_3K$ combination (Table 1, entries 1–5) we could observe that the continuous mode gave slightly lower yields compared to the P-US technique (entries 1 and 2, Table 1). $PhBF_3K$ is quite reactive and deboronylation was the main side reaction occurring, together with some extent of dehalogenation. These phenomena were most probably due to the high local pressure and temperature ('hot spots')[29] experienced by the substrates during cavitation, which could be also responsible for fast catalyst deactivation. These '*locally harsh conditions*' are probably less important during the milder pulsed-US protocol. This is further confirmed by the fact that C-US and P-US modes gave comparable yields after by fine-tuning the irradiation amplitude and the reaction time (entries 1 and 4, Table 1). It is also worthy of notice that the outcome of the reaction also depended on the amplitude of the irradiation (entries 3–5, Table 1). At 10% amplitude (entry 5), the yield was moderate and homocoupling product was detected in the crude, while at 40% amplitude (entry 3) deboronylation became important. Taking into account that comparable yields could be obtained with both C-US and P-US for these substrate combinations, we preferred to continue the investigation using the *'milder'* P-US method. With the more stable $PhB(OH)_2$, the reaction is not dependent on the amplitude (entries 7 and 8). As expected, reactions carried out in the absence of base (entries 6 and 9) and/or catalyst did not afford formation of any amount of the final product. With the *p*-bromoanisole/$PhBF_3K$ combination (Table 1, entries 10 and 11) the better results were obtained with P-US with respect to C-US, and other bases were tested (entries 12 and 13), being CsOH (entry 13) also effective, giving comparable results by prolonged irradiation. Moreover, under C-US (entry 10), the yield could not be improved extending the reaction times (up to 30 min), because deboronylation occurred in this case too. The same trend was observed also with the *p*-bromoanisole/$PhB(OH)_2$ combination (en-

Table 1. Screening of the reactions conditions for the Suzuki–Miyaura cross-coupling reaction under pulsed US.[a]

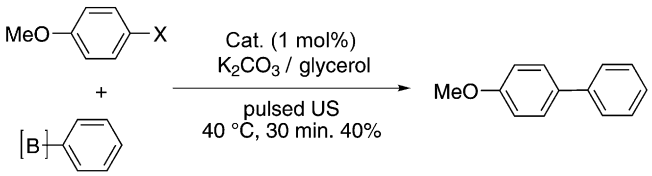

Entry	X	[B]	Base	t [min]-Method-A [%][b]	Yield [%][c]
1	I	BF_3K	K_2CO_3	30-P-40	79
2			K_2CO_3	30-C-40	61
3			K_2CO_3	10-C-40	58
4			K_2CO_3	10-C-20	76
5			K_2CO_3	10-C-10	57(5)[d]
6			–	10-C-40	0
7	I	$B(OH)_2$	K_2CO_3	30-P-40	83
8			K_2CO_3	30-P-20	85
9			–	30-P-40	0
10	Br	BF_3K	K_2CO_3	10-C-40	77
11			K_2CO_3	30-P-40	83
12			CsOAc	60-P-40	64
13			CsOH	60-P-40	84
14	Br	$B(OH)_2$	K_2CO_3	10-C-40	70
15			K_2CO_3	30-P-40	80
16	Cl	$B(OH)_2$	CsOH	30-P-40	48[e]

[a] Typically *p*-MeO-C_6H_4-X (X = I, Br, Cl) (0.25 mmol), boron source (0.375 mmol), base (0.875 mmol) and catalyst **1** (1 mol%) in glycerol (0.8 mL) were reacted in pulsed ultrasound (P-US) mode for 30 min.

[b] P = Pulsed mode (probe on for 10 sec – probe off for 10 sec), C = continuous mode, A = amplitude wave used.

[c] Yield was determined by ^1H NMR using CH_2Br_2 (0.25 mmol) as an internal standard and by GC using anisole (0.25 mmol) as reference.

[d] Homocoupling by-product.

[e] KI (30 mol%) was added.

tries 14 and 15). However, if the total reaction times in C-US (10 min) P-US (15 min) are similar, the cavitation may not be comparable in terms of local pressure and temperature,[29] or 'mechanical shocks'[30] experimented by the reactants.

Taking into account reaction kinetics, yields and the extent of conversion for each substrates/reaction conditions combination, we could affirm that halogenated anisoles reacted better when using potassium phenyltrifluoroboronate or phenylboronic acid keeping the ultrasound wave amplitude not below 20%. As a general trend, at lower amplitude values homocoupling by-products were observed, while the extent of deboronylation and dehalogentaion reactions increased at high amplitude values under continuous mode.

Under the optimized reaction conditions, no homocoupling or dehalogenation by-products were detected by ^{1}H NMR or GC; the catalyst was able to activate a full range of aryl halides, including *p*-chloroanisole, although only moderately in this case (48% yield, Table 1, entry 12). *p*-Chloroanisole was unreactive when using K_2CO_3 alone or in the presence of 30 mol% KI. The use of a stronger base such as KOH gave only traces of cross-coupling product, with CsOH alone, the GC yield was 5%. Better results were obtained using 30 mol% KI (Table 1, entry 12). If the quantity of KI was increased up to stoichiometric amount with respect to the substrate, again, reaction was inhibited.

Table 2 shows a comparative study of the catalytic performance of catalysts **1–4**, along with [$PdCl_2$(IPr)Py], [$Pd(AcO)_2$] and [$Pd(PPh_3)_4$], in the coupling of *p*-MeO-C_6H_4-Br and $PhBF_3K$. As observed, catalysts **1–4** afforded better yields than all three other Pd species (entries 5–7), and all four catalysts achieved full conversion in shorter reaction times, using a lower catalyst loading and milder temperature, than in previous reports.[14] The effect of both solvent and activation technique were also investigated (Table 3). Cross-coupling of *p*-bromoanisole and phenylboronic acid with catalysts **1–4** was performed in glycerol and the reaction mixture was heated (activated) using classic oil bath or pulsed US mode. With regard to the heating modes, it was important to take into account the low solubility of highly hydrophobic molecules in glycerol, and its high viscosity limiting mass transport capabilities.

Table 2. A comparative study under pulsed US activation.[a]

Entry	Cat.	Yield[b] [%]
1	**1**	83 (99)[c]
2	**2**	83
3	**3**	99
4	**4**	92 (99)[c]
5	PEPPSI-IPr	75
6	$Pd(OAc)_2$	68
7	$Pd(PPh_3)_4$	57

[a] Reaction were carried out with *p*-MeO-C_6H_4-Br (0.25 mmol), $PhBF_3K$ (0.375 mmol), K_2CO_3 (0.875 mmol) and palladium catalyst (1 mol%) in glycerol (0.8 mL), reacted in pulsed ultrasound (P-US, Amplitude 40%) mode for 30 min. (probe on for 10 sec – probe off for 10 sec) at 40 °C.

[b] Yield was determined by ^{1}H NMR using CH_2Br_2 (0.25 mmol) as an internal standard and by GC using anisole (0.25 mmol) as reference.

[c] Yield in parenthesis is given for *p*-iodoanisole as substrate.

Table 3. Study of the solvent influence and activation technique effects.[a]

Entry	Cat.	Yield[b,c] [%] after 30 min	
		Oil bath	Pulsed US
1	**1**	21 (44)	80
2	**2**	43 (89)	83
3	**3**	53 (98)	91
4	**4**	51 (96)	84

[a] Reactions were carried out with *p*-bromoanisole (0.25 mmol), Phenyl boronic acid (0.375 mmol), K_2CO_3 (0.875 mmol), 0.8 mL of glycerol at 40 °C.

[b] Yield was determined by ^{1}H NMR using CH_2Br_2 (0.25 mmol) as an internal standard and by GC using anisole (0.25 mmol) as reference.

[c] In parenthesis yields after 60 min reaction.

These limitations experienced under conventional heating modes were easily overcome by performing reactions under high intensity ultrasound (US) activation. In these conditions cavitation phenomena become important producing a microenvironment (micro bubbles) in which the reaction took place, affording high yields in all cases (Table 3).

The solubility test of catalysts **1–4** in glycerol revealed that the sulfonate-derived catalysts **3** and **4** are completely soluble, while catalysts **1** and **2** were only sparingly soluble (see Figure S1 of the Supporting Information). The catalytic activity observed in glycerol could be attributed to the formation of nanoparticles formed most probably by the polyol method[31,32] or by reduction of Pd(II) to Pd(0) by action of the boronic acids employed[33,34] (Figure 3). Stabilized by the ligands and/or by the solvent (glycerol), the nanoparticles remained small in size and did not agglomerate. We considered catalyst/solvent recycling. Unfortunately, recycling was not effective (Figure 3), except when the catalyst loading was increased (2 mol%), for catalyst **3**, which also was the one achieving the slowest deactivation rate. ICP-MS analyses showed that a small amount of palladium metal was detected in the filtrate after each run. Catalytic activity decreased after the first cycle. Leached palladium, or the presence of inorganic salts should be responsible for the decreased activity.

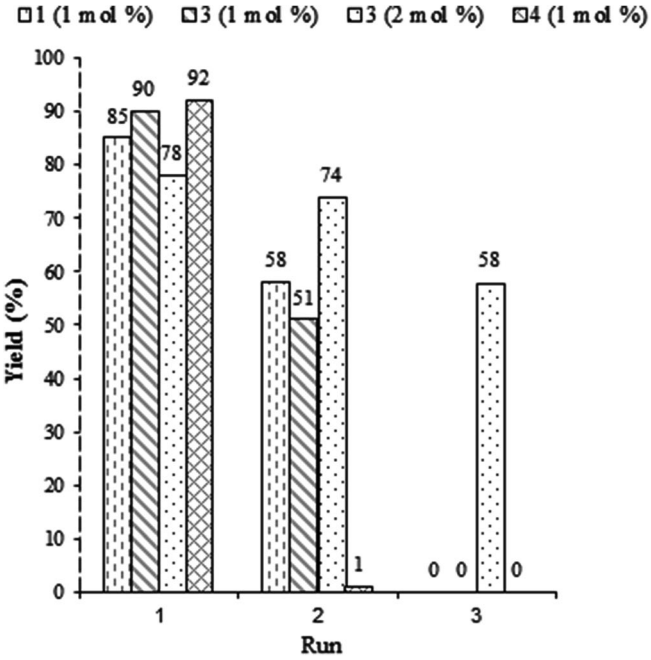

Residual Pd (ppm) by ICP-MS

Run	Cat. **1**[a,c] (1 mol%)	Cat. **3**[a,c] (1 mol%)	Cat. **4**[b,c] (1 mol%)	Cat. **3**[a,c] (2 mol%)
1	880	<50	<50	<300
2	60	<50	<300	<50
3	not performed	not performed	not performed	<180

[a] Reactions were carried out with *p*-iodooanisole (0.25 mmol), phenylboronic acid (0.375 mmol), K_2CO_3 (0.875 mmol), 0.8 mL of glycerol at 40 °C.

[b] Reactions were carried out with *p*-bromoanisole (0.25 mmol), potassium phenyltrifluoroboronate (0.375 mmol), K_2CO_3 (0.875 mmol), 0.8 mL of glycerol at 40 °C.

[c] P-US mode = probe on for 10 sec. – probe off for 10 sec.

Figure 3. Catalyst recycling in glycerol and residual palladium content extracted in the organic phase (ICP-MS analyses).

The methodology extended to other aryl halides and aryl boronic acids, revealed that the Suzuki–Miyaura cross coupling worked well with a range of bulky groups containing aryl halide or arylboronic acid substrates, affording good to excellent yields in all cases (Table 4). In particular, we selected everytime a different combination of aryl halide/boron source/catalyst without necessarily taking into account the steric and/or the electronic characteristics of each reactant, with the aim to demonstrate that independently of the catalyst or substrates, the reaction remained efficient. Both electron-rich and electron-poor aryl halides reacted with boron compounds leading to good to excellent yields, with all the catalysts chosen, independently also on the steric hindrance around the reactive sites. Only in one case, a moderate yield (68%, entry 9) was obtained when 5,5,8,8-tetramethyl-5,6,7,8-tetrahydronaphthalen-2-ylboronic acid reacted with 4-iodonitrobenzene. It is important to point out that the pure final products were recovered by a simple and practical work-up consisting in a decantation of the crude reaction mixture with glycerol immiscible solvents (e.g., Et_2O or cyclohexane). All the palladium catalysts were active in the Suzuki–Miyaura cross-coupling of 4-bromo-/4-iodoanisole and phenylboronic acid or potassium phenyltrifluroboronate using only 1 mol% catalyst and glycerol as the only solvent in a short time and open air atmosphere under pulsed US. Transmission electron microscopy (TEM) studies performed on the reaction mixtures obtained after the catalytic runs indicated the formation of palladium nanoparticles (Pd-NPs) under pulsed US activation in glycerol. Pd-NPs formation under similar conditions has recently been attributed to the reducing character of glycerol,[31] however, as previously mentioned, boronic acids can be also responsible for Pd(II) reduction.[33,34] In our case, we observed a different average size depending on catalyst/substrate combination (Figure 4). Moreover, for the same experiment, we observed that nanoparticles obtained under continuous US mode were less homogeneously dispersed than those coming from a pulsed US method, supporting the experimental evidence for a more efficient catalytic process in these conditions.

Both the nature and identity of the Pd-NPs were investigated by X-ray photoelectron spectroscopy (XPS) (Figure 5). As a reference, catalysts **1** and **3** were first analyzed. In the case of NHC-Pd(II) catalyst **1**, the binding energy of Pd electrons in the core $3d_{5/2}$ and $3d_{3/2}$ orbitals were displayed as two spectral lines at 337.0 eV and 342.3 eV, respectively, in agreement with results recently published, indicating the presence of NHC-Pd(II) species[35–37] (Figure 5, a, red spectrum). Pd-NPs XPS analyses originated by compound **1** showed the presence of two different palladium species in a 92:8 ratio. The major peak was a two component signal centered at 334.0 eV (for Pd $3d_{5/2}$) and 339.4 eV (for Pd $3d_{3/2}$). These values, at lower binding energy with respect to the NHC-Pd(II) in **1**, were consistent with a zero-valent palladium[38] species (Figure 5, a, green spectrum), in which the metal was in the 'naked' form (ligands were no longer present in the coordination sphere of the metal, as shown by the absence of N 1*s*, Cl 2*s* and $2p_{3/2}$ spectral lines). The minor peak at 335.7 eV (Pd $3d_{5/2}$) was assigned to PdO,[39] whose formation could be due to air Pd-NPs oxidation (post-operandum analysis). For catalyst **3**, as expected for a NHC-Pd(II),[35–37] the binding energy of Pd electrons in the core $3d_{5/2}$ orbitals was at 337.0 eV (Figure 5, b, red line),[24] with the S $2p_{3/2}$

Table 4. Substrate/catalyst scope for Suzuki–Miyaura coupling under pulsed ultrasound.[a]

Entry	R^1-X	R^2-B	Cat.	Product	Yield[b] [%]
1	4-MeO-C_6H_4-I	$PhB(OH)_2$	**1**	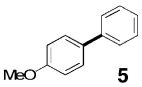 **5**	85[c]
2			**2**		86
3		$PhBF_3K$	**4**		82
4		naphthalene-1-boronic acid	**1**	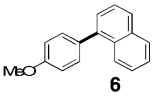 **6**	87[d]
5		3-Me-$C_6H_4B(OH)_2$	**1**	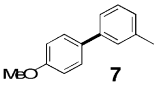 **7**	75
6	4-Me-C_6H_4-I	naphthalene-1-boronic acid	**3**	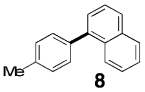 **8**	73[d]
7		$PhBF_3K$	**4**	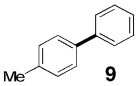 **9**	82
8	4-NO_2-C_6H_4-I	$PhB(OH)_2$	**3**	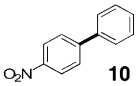 **10**	89[d]
9		5,5,8,8-tetramethyl-5,6,7,8-tetrahydronaphthalen-2-ylboronic acid	**2**	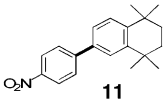 **11**	68[d]
10	9-iodophenanthrene	$PhBF_3K$	**1**	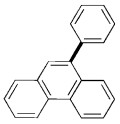 **12**	73
11	2-bromonaphthalene	3-Me-$C_6H_4B(OH)_2$	**3**	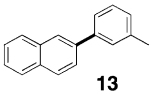 **13**	90
12	4-CHO-C_6H_4-Br	3-MeO-$C_6H_4B(OH)_2$	**4**	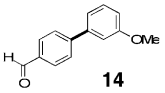 **14**	73
13	PhBr		**1**	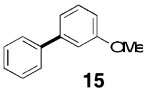 **15**	68

[a] Reactions were carried out with an aryl halide (0.25 mmol), a boron source (0.375 mmol), K_2CO_3 (0.875 mmol), 0.8 mL of glycerol at 40 °C, with 40% amplitude, for 30 min (pulsed US: 10 sec probe on/10 sec probe off).
[b] Yield was determined by ^1H NMR using CH_2Br_2 (0.25 mmol) as internal standard and by GC using anisole (0.25 mmol) as reference.
[c] Yield is given for 60 min reaction.
[d] Amplitude was 20 %.

peak centered at 166.9 eV, characteristic of a sulfonate group[36b] (Figure 5, c, red line). The deconvolution of the N 1*s* peak accounted for the presence of nitrogen atoms surrounded by different chemical environments assigned to the NHC ligand (399.6 eV) and to the pyridine (400.8 eV) in a Pd/N 1:3 ratio. The analysis of Pd(0)-NPs obtained after reaction revealed a modification of Pd/N and Pd/S ratios and the presence of two different Pd(0) species in a measured 1:4 ratio. The minor peak at 333.9 eV (Pd $3d_{5/2}$) was assigned to a bulk metal Pd(0), while the major peak at 335.8 eV was attributed to a possible species where the sulfonate group acted as a palladium ligand (Figure 5, b and Figure 6). The S $2p_{3/2}$ peak shifted to a lower binding energy (163.2 eV) (Figure 5, c, green line) might be due to the formation of a bond between the oxygen and the metal, as suggested in Figure 6, showing that the NHC ligand partially remained in the coordination sphere of the metal.[24]

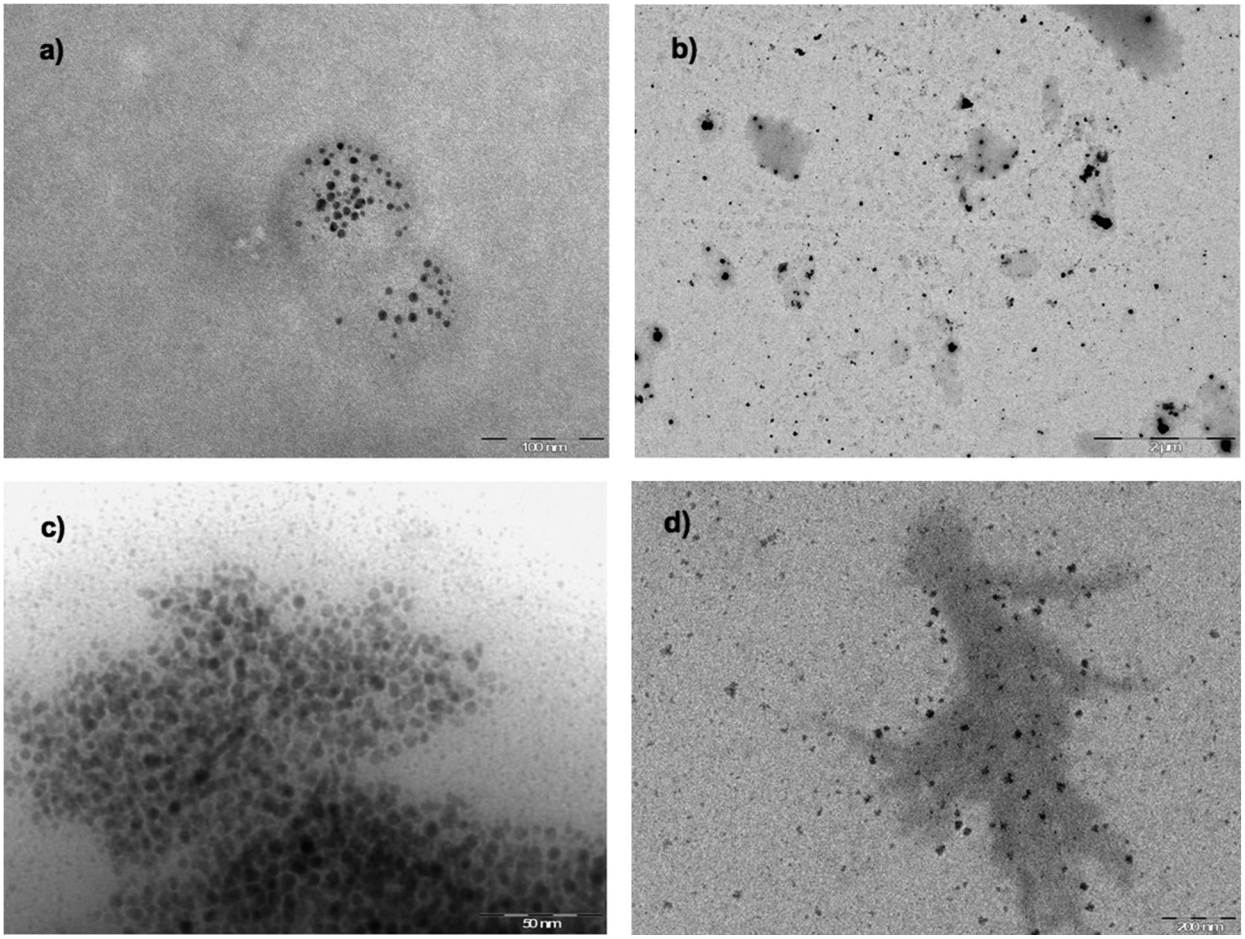

Figure 4. TEM micrographs of glycerol phase (post-reaction mixture) for the Suzuki–Miyaura reaction of potassium trifluoroborate with: a) **1** and *p*-iodoanisole under pulsed US mode, Pd-NPs average size *ca.* 5–7 nm; b) **1** and *p*-iodoanisole under continuous US mode; c) **2** and *p*-bromoanisole, under pulsed US Pd-NPs average size ca. 3-4 nm; d) **3** and *p*-bromoanisole, under pulsed US Pd-NPs average size *ca.* 17–21 nm.

Conclusions

Four new Pd-NHC-based complexes have been synthesized and fully characterized. Their catalytic properties were evaluated and compared, in the Suzuki–Miyaura cross-coupling, using glycerol as solvent under pulsed ultrasound, which gains a special place as a promising activation technique for developing new catalytic processes in glycerol. Catalyst fate was investigated through TEM and XPS analyses. Whether if rigidly classifying the transformation as a homogenous or heterogeneous process, we preferred to fill the gap postulating that different active catalytic species ('*cocktail of compounds*')[40] were present in solution. This supported the experimental evidence for a different catalytic pathway of catalysts **1–4** with respect to PEPPSI-IPr. The question for a unified concept of catalysis involving a heterogenization-homogenization pathway remains to be answered on the basis of the actual knowledge and it is still under debate in the scientific community.[41] Due to its industrial importance as the intermediate of a large range of valuable fine chemicals, as well as the solvent of choice for many industrial and pharmaceutical preparations (foods, cosmetics, liquid detergents, antifreeze compounds), new methodologies are being developed in our laboratory for a green and sustainable chemistry with glycerol.

Experimental Section

General Method for the Suzuki–Miyaura Reaction under Pulsed US

In a typical experiment, a mixture of substrate (0.25 mmol), boronic acid or boronate salt (0.375 mmol), catalyst (1 mol%), K_2CO_3 (0.875 mmol) in glycerol (0.8 mL) was placed in a Pyrex® glass reactor and clamped to a vertical support on a magnetic stirrer. The vessel was held in place to allow immersion of the tip horn into the reaction mixture to a depth of 1.0 cm and the glass part not touching the sonochemical probe. The reaction was sonicated at 40 °C for

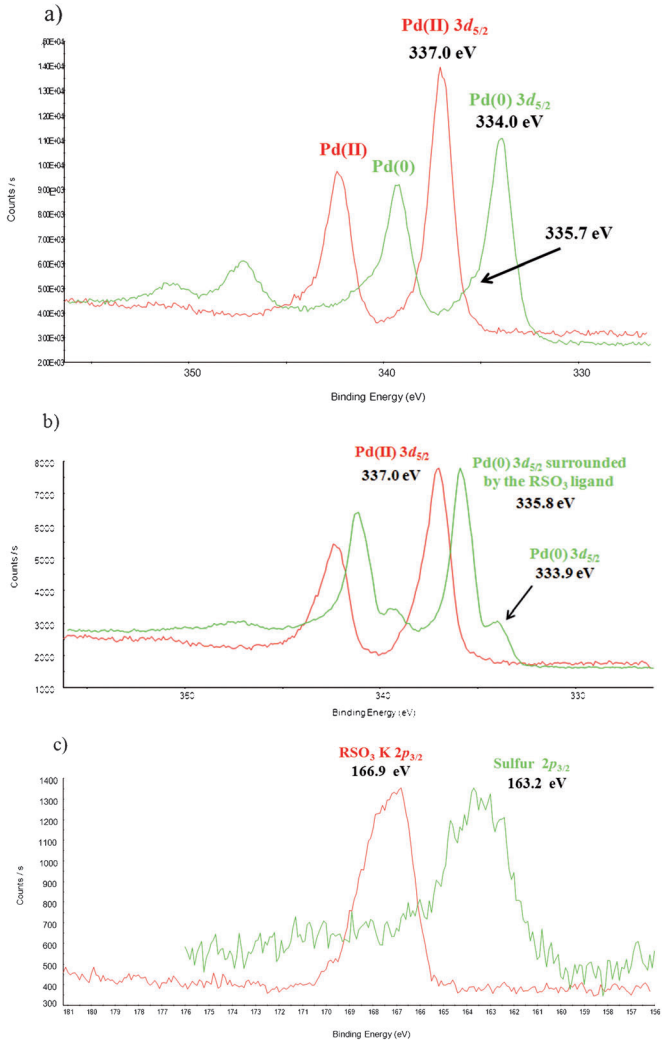

Figure 5. XPS spectra for: a) catalyst **1** before reaction (red line) and Pd-NPs in glycerol after reaction (green line) using pulsed US with *p*-iodoanisole (Table 1, entry 1); b) catalyst **3** before reaction (red line) and Pd-NPs in glycerol after reaction (green line) using pulsed US with *p*-bromoanisole (Table 2, entry 3); c) sulfur in catalyst **3** before reaction (red line) and in Pd-NPs in glycerol after reaction (green line).

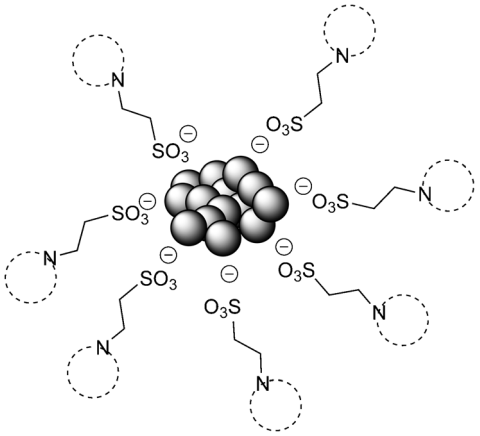

Figure 6. Model for Pd-NPs with RSO_3^- ligand.

30 min (probe on for 10 sec – probe off for 10 sec) with 40% wave amplitude, while keeping vigorous magnetic stirring. At the end of the reaction, a mixture 2:1 v/v of Et_2O/CH_2Cl_2 (3 mL) was added to the crude and stirring was continued for 5 min at room temperature. The supernatant was recovered and the operation was repeated three times. The organic phase was dried over $MgSO_4$, filtered and evaporated under reduced pressure to afford the expected cross-coupling product as a pure compound. Product conversion was determined by HPLC; yield was determined by GC/MS and ^{1}H NMR.

General Procedure to Recycle the Catalytic System

A typical experimental procedure to recycle the catalytic system constituted by metal and glycerol is described. The glycerol phase from the previous run was maintained for 5 h under dynamic vacuum while stirring. Then, the aryl halide (0.25 mmol) and the arylboronic acid or potassium phenyltrifluoroborate (0.375 mmol) were added to the glycerol phase. The mixture was sonicated (pulsed method) for 30 min in the same conditions as for the first run, to afford pure cross-coupling product after usual work-up.

Synthesis of 1

A mixture of the imidazolium salt **A** (190 mg, 0.56 mmol), $PdCl_2$ (100 mg, 0.56 mmol), and K_2CO_3 (154 mg, 1.12 mmol) was stirred at 60 °C for 12 h under argon, using pyridine as solvent. After cooling to room temperature the resulting mixture was filtered through celite, and the filtrate was concentrated to dryness. The residue was crystallized in CH_2Cl_2/hexane mixture. The solid obtained was dried under vacuum affording a clear yellow product; yield: 0.240 g (75%). ^{1}H NMR ($CDCl_3$, 300 MHz): $\delta = 9.05$–8.95 (m, 2H, Py), 7.81 (t, 1H, Py), 7.38–7.33 (m, $J = 7.6$, 6.5 Hz, 2H, Py), 6.92 (d, $J = 2.1$ Hz, 1H, Ar), 6.78 (d, $J = 2.2$ Hz, 3H, ArH_{imid}), 5.76 (s, 2H, NCH_2), 4.63 (t, 2H, NCH_2), 3.85 (s, 6H, OCH_3), 3.84 (s, 3H, OCH_3), 2.13–2.06 (m, $J = 15.2$, 7.7 Hz, 2H, NCH_2CH_2), 1.53–1.44 (m, 2H, $NCH_2CH_2CH_2$), 1.04 (t, $^3J_{H,H} = 7.4$ Hz, 3H, CH_3); ^{13}C NMR ($CDCl_3$, 125 MHz): $\delta = 153.5$ ($C_{carbene}$), 151.2, 138.4 (Py), 138.1, 131.1 (Ar), 124.9 (Py), 124.4, 122.1 (CH_{imid}), 105.9 (Ar), 60.7, 56.4 (OMe), 54.8 (NCH_2Ar), 50.8, 32.5, 19.91, 13.7 (*n*-Bu); anal. calcd. for $C_{22}H_{29}N_3PdCl_2O_3$ (560.81): C 47.12, H 5.21, N 7.49; found: C 46.80, H 5.33, N, 7.66; electrospray MS. (cone 20 V): *m/z* (fragment) = 526.1 $[M-Cl]^+$, 488.1 $[M-Cl-Py+CH_3CN]^+$, 447.1 $[M-Cl-Py]^+$; HR-MS (ESI-TOF-MS, positive mode): *m/z* = 447.0510, monoisotopic peak, calcd. $[M-Cl-Py]^+$: 447.0508, ε_r: 0.4 ppm.

The crystal structure of complex **1** has been deposited at the Cambridge Crystallographic Data Centre and allocated the deposition number CCDC 911242. These data can be obtained free of charge from The Cambridge Crystallographic Data Centre *via* www.ccdc.cam.ac.uk/data_request/cif.

Synthesis of 2

A mixture of the imidazolium salt **B** (271 mg, 0.58 mmol), $PdCl_2$ (70 mg, 0.39 mmol), and K_2CO_3 (107 mg, 0.78 mmol) was stirred at 60 °C for 12 h under argon, using pyridine as solvent. After cooling to room temperature the resulting

mixture was filtered through celite, and the filtrate was concentrated to dryness. The residue was crystallized in CH_2Cl_2/hexane mixture. The yellowish solid obtained was dried under vacuum; yield: 0.229 g (86%). ^{1}H NMR ($CDCl_3$, 300 MHz): δ = 9.07–8.99 (m, 2H, Py), 7.80 (t, $^3J_{H,H}$ = 7.6 Hz, 1H, Py), 7.43–7.33 (m, 2H, Py), 6.83 (s, 4H, Ar), 6.81 (d, J = 0.7 Hz, 2H, H_{imid}), 5.82 (s, 4H, NCH_2), 3.88 (d, J = 0.6 Hz, 12H, OCH_3), 3.86 (d, J = 0.8 Hz, 6H, OCH_3); ^{13}C NMR ($CDCl_3$, 75 MHz): δ = 153.6 ($C_{carbene}$), 151.2, 138.1 (Py), 131.0 (Ar), 124.5 (Py), 121.9 (CH_{imid}), 106.0 (Ar), 60.8, 56.4 (OMe), 54.9 (NCH_2Ar); anal. calcd. for $C_{28}H_{33}N_3PdCl_2O_6$ (684.91): C 49.10, H 4.86, N, 6.14; found: C 49.50, H 5.03, N, 6.16; electrospray MS (cone 20 V): m/z (fragment) = 648.2 $[M-Cl]^+$, 571.1 $[M-Cl-Py]^+$; HR-MS (ESI-TOF-MS, positive mode): m/z = 571.0673, monoisotopic peak, calcd. for $[M-Cl-Py]^+$: 571.0670, ε_r: 0.5 ppm.

Synthesis of 3

A mixture of *N,N′*-(butyl)(propanesulfonate)imidazolium salt **C** (151 mg, 0.616 mmol), $PdCl_2$ (100 mg, 0.56 mmol), and K_2CO_3 (154 mg, 1.12 mmol) was stirred at 60 °C for 12 h under Ar, using pyridine as solvent. After cooling to room temperature the resulting mixture was filtered through celite, and the filtrate was concentrated to dryness. The residue was purified by silica gel column chromatography. The second band eluting with 1:1 acetone-MeOH (v/v) was collected, the solvent evaporated and the solid residue dried under vacuum to afford a yellow solid product; yield: 0.18 g (60%). ^{1}H NMR (MeOD, 300 MHz): δ = 8.88 (d, J = 5.2 Hz, 2H, Py), 7.91 (t, $^3J_{H,H}$ = 7.7 Hz, 1H, Py), 7.49–7.43 (m, 2H, Py), 7.32 (d, J = 1.3 Hz, 1H, H_{imid}), 7.23 (d, J = 1.4 Hz, 1H, H_{imid}), 4.72 (t, $^3J_{H,H}$ = 7.1 Hz, 2H, NCH_2), 4.52 (t, $^3J_{H,H}$ = 7.5 Hz, 2H, NCH_2), 2.94 (t, $^3J_{H,H}$ = 7.2 Hz, 2H, -CH_2SO_3), 2.63 (quint., J = 7.1 Hz, 2H, -$CH_2CH_2SO_3$), 2.17–2.02 (quint, 2H,), 1.47 (sext, J = 14.9, 7.5 Hz, 2H, $CH_2CH_2CH_2CH_3$), 1.04 (t, $^3J_{H,H}$ = 7.3 Hz, 3H, CH_3). ^{13}C NMR ($CDCl_3$, 75 MHz): δ = 152.8 ($C_{carbene}$), 151.2, 138.8, 124.9(Py), 123.1, 122.5(CH_{imid}), 50.7, 32.7, 19.8, 13.2 (*n*-Bu), 26.7($CH_2CH_2SO_3$); anal. calcd. for $C_{15}H_{22}N_3PdCl_2SO_3K$ (540.85): C 33.31, H 4.10, N 7.77; found: C 33.70, H 4.18, N 7.66; electrospray MS (cone 15 V, negative mode): m/z (fragment) = 502.0 $[M]^-$, 422.9 $[M-Py]^-$; HR-MS (ESI-TOF-MS, negative mode): m/z = 422.9365 monoisotopic peak, calcd. for $[M-Py]^-$: 422.9362, ε_r: 0.7 ppm.

Synthesis of 4

A mixture of *N,N′*-(methyl)(propanesulfonate)imidazolium salt **D** (87 mg, 0.43 mmol), $PdCl_2$ (70 mg, 0.39 mmol), and K_2CO_3 (107 mg, 0.78 mmol) was stirred at 60 °C for 12 h under argon, using pyridine as solvent. After cooling to room temperature the resulting mixture was filtered through celite, and the filtrate was concentrated to dryness. The residue was purified by silica gel column chromatography. Eluting with acetone-MeOH (1:1 v/v) afforded a yellowish crystalline product; yield: 0.112 g (58%). ^{1}H NMR (MeOD, 300 MHz): δ = 8.89 (d, J = 5.1 Hz, 2H, Py), 7.91 (t, $^3J_{H,H}$ = 7.5 Hz, 1H, Py), 7.53–7.41 (m, 2H, Py), 7.32 (d, J = 1.9 Hz, 1H, H_{imid}), 7.21 (d, J = 1.9 Hz, 1H, H_{imid}), 4.71 (t, $^3J_{H,H}$ = 7.1 Hz, 2H, NCH_2), 4.10 (s, 3H,NCH_3), 2.94 (t, $^3J_{H,H}$ = 7.2 Hz, 2H, CH_2SO_3), 2.62 (p, J = 7.2 Hz, 2H, NCH_2CH_2); ^{13}C NMR ($CDCl_3$, 75 MHz): δ = 152.1 ($C_{carbene}$), 150.8, 139.7, 125.8 (Py), 124.6, 123.6 (CH_{imid}), 38.0 (NCH_3), 27.4 ($CH_2CH_2SO_3$); anal. calcd. for $C_{12}H_{16}N_3SO_3PdCl_2K$ CH_3COCH_3 (556.85): C 32.35, H 3.98, N, 7.55; found: C 32.19, H 3.77, N 7.59; electrospray MS (cone 20 V, negative mode): m/z (fragment) = 459.9 $[M]^-$, 380.9 $[M-Py]^-$; HR-MS (ESI-TOF-MS, negative mode): m/z = 380.8896 monoisotopic peak, calc. for $[M-Py]^-$: 380.8892, ε_r: 1.0 ppm.

Acknowledgements

We thank for financial support the Ministerio de Ciencia e Innovación of Spain (CTQ2011-24055/BQU) and Bancaixa (P1.1B2010-02), the French CNRS and MESR. A. A. is grateful to 'Generalitat Valenciana' for a Ph.D. fellowship. The authors are grateful to the Serveis Centrals d'Instrumentació Científica (SCIC) (for spectroscopic facilities, Universitat Jaume I – Spain), Franck Godiard (for TEM analyses, 'Service de Microscopie Electronique et Analytique', Université Montpellier II – France); Valérie Flaud (for XPS data) and Dr. Clarence Charnay (Institut Charles Gerhardt, Montpellier – France) for fruitful discussions.

References

[1] P. T. Anastas, J. Warner, in: *Green Chemistry: Theory and Practice*, Oxford University Press, Oxford, **1998**.
[2] P. T. Anastas, M. M. Kirchhoff, *Acc. Chem. Res.* **2002**, *35*, 686.
[3] F. M. Kerton, in: *Alternative Solvents for Green Chemistry*, RSC Green Chemistry Series, (Series Ed.: J. Clark), **2009**.
[4] R. B. N. Baig, R. S. Varma, *Chem. Soc. Rev.* **2012**, *41*, 1559–1584.
[5] C. O. Kappe, *Chem. Soc. Rev.* **2008**, *37*, 1127–1139.
[6] G. Cravotto, P. Cintas, *Chem. Soc. Rev.* **2006**, *35*, 180–196.
[7] Y. L. Gu, F. Jerome, *Green Chem.* **2010**, *12*, 1127–1138.
[8] N. Bakhrou, F. Lamaty, J. Martinez, E. Colacino, *Tetrahedron Lett.* **2010**, *51*, 3935–3937.
[9] A. Azua, J. A. Mata, E. Peris, F. Lamaty, J. Martinez, E. Colacino, *Organometallics* **2012**, *31*, 3911–3919.
[10] M. Pagliaro, R. Ciriminna, H. Kimura, M. Rossi, C. Della Pina, *Angew. Chem.* **2007**, *119*, 4516–4522; *Angew. Chem. Int. Ed.* **2007**, *46*, 4434–4440.
[11] M. Pagliaro, M. Rossi, in: *The Future of Glycerol*, 2nd edn., RSC Publishing, Cambridge, **2010**, p 170.
[12] A. E. Diaz-Alvarez, J. Francos, B. Lastra-Barreira, P. Crochet, V. Cadierno, *Chem. Commun.* **2011**, *47*, 6208–6227.
[13] A. Wolfson, C. Dlugy, *Chem. Pap.* **2007**, *61*, 228–232.
[14] G. Cravotto, L. Orio, E. Calcio Gaudino, K. Martina, D. Tavor, A. Wolfson, *ChemSusChem* **2011**, *4*, 1130–1134.
[15] C. J. O'Brien, E. A. Kantchev, C. Valente, M Hadei, G. Chas, A. Lough, A. C. Hopkinson, M. G. Organ, *Chem. Eur. J.* **2006**, *12*, 4743.
[16] M. G. Organ, S. Avola, I. Dubovyk, N. Hadei, E. A. B. Kantchev, C. J. O'Brien, C. Valente, *Chem. Eur. J.* **2006**, *12*, 4749–4755.

[17] C. Valente, M. E. Belowich, N. Hadei, M. G. Organ, *Eur. J. Org. Chem.* **2010**, 4343–4748.
[18] M. G. Organ, M. Abdel-Hadi, S. Avola, I. Dubovyk, N. Hadei, E. A. B. Kantchev, C. J. O'Brien, M. Sayah, C. Valente, *Chem. Eur. J.* **2008**, *14*, 2443–2452.
[19] M. G. Organ, S. Calimsiz, M. Sayah, K. H. Hoi, A. J. Lough, *Angew. Chem.* **2009**, *121*, 2419–2423; *Angew. Chem. Int. Ed.* **2009**, *48*, 2383–2387.
[20] J. Nasielski, N. Hadei, G. Achonduh, E. A. B. Kantchev, C. J. O'Brien, A. Lough, M. G. Organ, *Chem. Eur. J.* **2010**, *16*, 10844–10853.
[21] A. Azua, S. Sanz, E. Peris, *Organometallics* **2010**, *29*, 3661–3664.
[22] H. Ohta, T. Fujiharaa, Y. Tsuji, *Dalton Trans.* **2008**, 379–385.
[23] M. Yoshizawa-Fujita, T. Tamura, Y. Takeoka, M. Rikukawa, *Chem. Commun.* **2011**, *47*, 2345–2347.
[24] See the Supporting Information.
[25] P. Nun, J. Martinez, F. Lamaty, *Synlett* **2009**, 1761–1764.
[26] A. Azua, J. A. Mata, E. Peris, *Organometallics* **2011**, *30*, 5532–5536.
[27] M. Poyatos, J. A. Mata, E. Peris, *Chem. Rev.* **2009**, *109*, 3677–3707.
[28] D. Canseco-Gonzalez, A. Gniewek, M. Szulmanowicz, H. Müller-Bunz, A. M. Trzeciak, M. Albrecht, *Chem. Eur. J.* **2012**, *18*, 6055–6062.
[29] G. Cravotto, P. Cintas, *Chem. Sci.* **2012**, *3*, 295–307.
[30] G. Cravotto, P. Cintas, *Angew. Chem.* **2007**, *119*, 5573–5575; *Angew. Chem. Int. Ed.* **2007**, *46*, 5476–5478.
[31] A. N. Grace, K. Pandian, *Mater. Chem. Phys.* **2007**, *104*, 191–198.
[32] S. Komarneni, D. Li, B. Newalkar, H. Katsuki, S. Bhalla, *Langmuir* **2002**, *18*, 5959–5962.
[33] E. Tomás-Mendivil, J. Díez, V. Cadierno, *Catal. Sci. Technol.* **2011**, *1*, 1605–1615.
[34] L. A. Adrio, B. N. Nguyen, G. Guilera, A. G. Livingston, K. K. Hii, *Catal. Sci. Technol.* **2012**, *2*, 316–325.
[35] D. H. Lee, J. H. Kim, H. J. Kang, J. Park, Y. S. Lee, *Org. Lett.* **2008**, *10*, 1609–1612.
[36] T. Yu, Y. Li, C. Yao, H. Wu, Y. Liu, P. Wu, *Chin. J. Catal.* **2011**, *32*, 1712–1718.
[37] G. Liu, M. Hou, T. Wu, T. Jiang, H. Fan, G. Yang, B. Han, *Phys. Chem. Chem. Phys.* **2011**, *13*, 2062–2068.
[38] a) J. F. Moulder, W. F. Stickle, P. E. Sobol, K. D. Bomben, *Handbook of X-ray Photoelectron Spectroscopy*, Perkin-Elmer, Waltham, MA, **1992**; b) literature data for $PhSO_3Na$: S $2p_{3/2}$ at 167.9 eV.
[39] M. Brun, A. Berthet, J. C. Bertolini, *J. Elec. Spectr. Rel. Phenom.* **1999**, *104*, 55–60.
[40] V. P. Ananikov, I. P. Beletskaya, *Organometallics* **2012**, *31*, 1595–1604.
[41] R. H. Crabtree, *Chem. Rev.* **2012**, *112*, 1536–1554.

